J|A|C|S
ARTICLES
Published on Web 06/05/2007

Intracrystalline Diffusivities and Surface Permeabilities Deduced from Transient Concentration Profiles: Methanol in MOF Manganese Formate

Pavel V. Kortunov,[†,‡] Lars Heinke,[†] Mirko Arnold,[§] Yannic Nedellec,[||] Deborah J. Jones,[||] Jürgen Caro,[§] and Jörg Kärger*[,†]

Contribution from the Universität Leipzig, Linnéstr. 5, 04103 Leipzig, Germany, Corporate Strategic Research, ExxonMobil Research and Engineering Company, 1545 Route 22 East, Annandale, New Jersey 08801, Leibniz Universität Hannover, Callinstr. 3-3A, 30167 Hannover, Germany, and Université Montpellier 2, Place E. Bataillon, 34095 Montpellier CEDEX 5, France

Received February 27, 2007; E-mail: kaerger@physik.uni-leipzig.de

Abstract: The intracrystalline concentration profiles during molecular uptake of methanol by an initially empty, single crystal of microporous manganese(II) formate ($Mn(HCO_2)_2$), representing an ionic inorganic−organic hybrid within the MOF family, are monitored by interference microscopy. Within these profiles, a crystal section could be detected where over the total of its extension ($\approx 2\ \mu m \times 50\ \mu m \times 30\ \mu m$) molecular uptake ideally followed the pattern of one-dimensional diffusion. Analysis of the evolution of intracrystalline concentration in this section directly yields the permeability of the crystal surface and the intracrystalline diffusivity as a function of the concentration of the total range of $0 \leq \theta \leq 0.57$ covered in the experiments. Within this range, the surface permeability is found to increase by 1 order of magnitude, while, within the limits of accuracy (±30%), the transport diffusivity remains constant, thus reflecting the properties of the lattice gas model.

Introduction

In many cases of their technical applications in catalysis[1] and mass separation[2] and as novel opto-electronic devices,[3] the performance of nanoporous material is controlled by their transport properties. Over decades, relevant information could only be obtained by macroscopic methods, i.e., by measurements with beds of crystallites/particles or, at best, with individual crystallites revealing the average response curves of uptake/release on the individual molecules. The introduction of pulsed field gradient nuclear magnetic resonance (PFG NMR,[4−6] in the seventies) and quasi-elastic neutron scattering (QENS,[7] in the eighties) to zeolite science and technology allowed the direct observation of molecular displacements which were small enough (micrometers in PFG NMR, nanometers in QENS) to provide direct information about the translational intracrystalline mobility. However, only recently, also the observation of intracrystalline transport diffusion has become possible. In coherent QENS experiments[8,9] (using, e.g., deuterium rather than protons as scatterers) transport diffusivities are determined by measuring the correlation times of the local fluctuation of intracrystalline concentration. Interference microscopy, which has recently been introduced to diffusion studies of zeolites,[10] allows us to record the evolution of intracrystalline concentration profiles during molecular uptake and release. As a most remarkable finding of these studies, in many cases the actual intracrystalline concentration profiles turned out to be notably different from the patterns which one would have expected on the basis of the data resulting for the average uptake/release by applying the conventional scheme of data analysis.[11] In many cases substantial differences between the actual habit of the zeolite crystal under study and the ideal (textbook) structure were identified as the origin of these complications. In the present study, interference microscopy is for the first time applied to a member of the MOF family. With methanol as a probe molecule, molecular uptake by an (initially empty, i.e., "activated") crystal of manganese(II) formate ($Mn(HCO_2)_2$) during a pressure step from 0 to 10 mbar in the surrounding atmosphere is followed. It shall be shown that the transient

[†] Universität Leipzig.
[‡] ExxonMobil Research and Engineering Company.
[§] Leibniz Universität Hannover.
[||] Université Montpellier 2.

(1) Chen, N. Y.; Degnan, T. F.; Smith, C. M. *Molecular Transport and Reaction in Zeolites*; VCH: New York, 1994.
(2) Kuznicki, S. M. *Nature* **2001**, 720−724.
(3) Davis, M. E. *Nature* **2002**, *417*, 813−821.
(4) Stejskal, E. O.; Tanner, J. E. *J. Chem. Phys.* **1965**, *42*, 288.
(5) Kärger, J.; Pfeifer, H.; Heink, W. *Adv. Magn. Reson.* **1988**, *12*, 2−89.
(6) Callaghan, P. T. *Aust. J. Phys.* **1984**, *37*, 359−387.
(7) Jobic, H.; Bee, M.; Caro, J.; Bülow, M.; Kärger, J. *J. Chem. Soc., Faraday Trans. I* **1989**, *85*, 4201−4209.
(8) Jobic, H.; Skoulidas, A. I.; Sholl, D. S. *J. Phys. Chem. B* **2004**, *108*, 10613−10616.
(9) Jobic, H.; Kärger, J.; Bee, M. *Phys. Rev. Lett.* **1999**, *82*, 4260−4263.
(10) Schemmert, U.; Kärger, J.; Weitkamp, J. *Microporous Mesoporous Mater.* **1999**, *32*, 101−110.
(11) Kortunov, P.; Chmelik, C.; Kärger, J.; Rakoczy, R. A.; Ruthven, D. M.; Traa, Y.; Vasenkov, S.; Weitkamp, J. *Adsorption* **2005**, *11*, 235−244.

profiles observed provide direct evidence that over the whole range of concentration (from zero to more than one-half of pore saturation) the transport diffusivity remains constant. In the following theoretical section we provide a short review that this behavior is exactly the pattern to be expected for systems which follow the simple model of a lattice gas. The subsequent Experimental Section introduces the application of interference microscopy to diffusion studies in nanoporous crystals, together with a description of the experiments performed. Finally, on presenting and discussing the results, we shall demonstrate that the observed transient concentration profiles are controlled by the combined influence of intracrystalline diffusion and surface barriers. The obtained diffusivities are found to be constant, following the behavior to be expected on the basis of the lattice gas model. By contrast, the permeability through the crystal surface increases by an order of magnitude.

Theory: The Lattice Gas Model

There is scarcely another, equally straightforward conception which so efficiently and sustainably contributed to our rationalization of molecular adsorption and diffusion on surfaces and porous media like the lattice-gas model.[12] In this model, the sorbate−sorbent interaction (i.e., the interaction between the guest molecules and the solid host) is assumed to give rise to molecular distributions on lattice points where the guest−guest interaction is taken account of by the sole requirement that at one and the same instant of time no more than one guest molecule is able to occupy a particular lattice point.[13−16] In the simplest case, the molecules are distributed over a rectangular network of equivalent lattice points of separation l. $dt/(2n\tau)$ denotes the probability that during a time interval dt a molecule will perform a jump attempt to a particular one of the adjacent sites. $n = 1$, 2, or 3 denotes the dimensionality of the network. A jump attempt is assumed to be only successful if the site to which it is directed is empty. Thus, τ turns out to be the mean life time between subsequent jumps for an isolated particle on the lattice.

These model assumptions may be easily developed to an estimate of two properties of the host−guest system which are crucial for their technical application in catalysis[1] and mass separation[2] and as novel opto-electronic devices,[3] namely their adsorption capacity and the rate of their internal dynamics.

The relative amount adsorbed by the host system at a given pressure p of guest molecules in the surrounding atmosphere coincides with the probability Θ that a lattice point is occupied by a guest molecule. Dynamic equilibrium requires equality of the number of guest molecules leaving and occupying lattice sites in identical time intervals. Applying this reasoning to boundary sites, i.e., to lattice sites in direct exchange with the surrounding atmosphere, yields

$$k_a\, p(1-\theta) = k_d\theta \tag{1}$$

which may be rearranged to

$$\theta = \frac{\kappa\, p}{1+\kappa\, p} \tag{2}$$

with k_d and $k_a\, p$ denoting, respectively, the molecular escape rate from an occupied boundary site and the occupation rate by a vacant boundary site at pressure p. In this way, close to one century ago,[17] the simple "Langmuir-type" adsorption isotherm has been introduced, with the ratio $\kappa = k_a/k_d$ as the only free parameter of the equation. Though the details of adsorption by nanoporous materials, in general, need a more complex treatment[14,18] for numerous systems, the Langmuir isotherm has served as an invaluable first tool to quantify the adsorption properties of porous media.[19]

The implications of the lattice gas model to molecular diffusion in complex systems are extensively discussed in the current literature.[12,20] The treatment becomes straightforward for single-component diffusion in one direction. In this case, the flux density j_y in the y-direction between sites at position y and $y + l$ is simply the net effect of molecular jumps from y to $y + l$ and vice versa, from $y + l$ to y, leading to

$$j_y = \frac{c_{site}\, l}{2\tau}\{\theta(y)[1-\theta(y+l)] + \theta(y+l)[1-\theta(y)]\} = -c_{site}\frac{l^2}{2\tau}\frac{d\theta}{dy} \tag{3}$$

where c_{site} denotes the number of sites per volume. Hence, $c_{site}\Theta$ is nothing else than the concentration of guest molecules so that the right-hand part of eq 3 is easily identified as Fick's first law.[1,21] The transport diffusivity results as the factor of proportionality

$$D_T = \frac{l^2}{2\tau} \tag{4}$$

which turns out to be independent of the loading since, within the lattice gas model, the quantities l and τ are constant.

By contrast, uptake and release measurements with nanoporous solids[22] are often found to exhibit notable concentration dependences. Hence, for convenience, in adsorption science and technology the transport diffusivity is generally replaced by the so-called corrected diffusivity

$$D_0 = \frac{\partial \ln \theta}{\partial \ln p} D_T \tag{5}$$

(12) Kehr, K. W.; Mussawisade, K.; Schütz, G. M.; Wichmann, T. In *Diffusion of Particles on Lattices*; Heitjans, P., Kärger, J., Eds.; Springer: Berlin, 2005; p 975.
(13) Saravanan, C.; Jousse, F.; Auerbach, S. M. *Phys. Rev. Lett.* **1998**, *80*, 5754−5757.
(14) Keil, F. J.; Krishna, R.; Coppens, M. O. *Rev. Chem. Eng.* **2000**, *16*, 71−197.
(15) Ramanan, H.; Auerbach, S. M.; Tsapatsis, M. *J. Phys. Chem. B* **2004**, *108*, 17171−17178.
(16) Snurr, R. Q.; Bell, A. T.; Theodorou, D. N. *J. Phys. Chem.* **1994**, *98*, 11948−11961.
(17) Langmuir, I. *J. Am. Chem. Soc.* **1918**, *40*, 1361.
(18) Myers, A. L. *Adsorption* **2003**, *9*, 9−16.
(19) Schüth, F.; Sing, K. S. W.; Weitkamp, J. *Handbook of Porous Solids*; Wiley-VCH: Weinheim, 2002.
(20) Kutner, R.; Pekalski, A.; Sznajd-Weron, K. *Anomalous Diffusion: From Basics to Applications*; Springer: Berlin, 1999.
(21) Kärger, J.; Ruthven, D. M. *Diffusion in Zeolites and Other Microporous Solids*; Wiley & Sons: New York, 1992.
(22) Ruthven, D. M. *Principles of Adsorption and Adsorption Processes*; Wiley: New York, 1984.

which, in many cases,[23−25] turns out to be much less dependent on concentration than the transport diffusivity. The first term on the right-hand side of eq 5 is referred to as the thermodynamic factor and is a measure of the deviation of the adsorption isotherm $\theta(p)$ from proportionality between loading and pressure.

In fact, for the analytic solution of diffusion problems very often the concentration dependence of the transport diffusivity is simply assumed as to be given by the thermodynamic factor, while D_0 is implied to be constant[23] (see also p 245 of ref 21).

For the lattice gas, these generally presumed trends in the concentration dependence are reversed. Now, D_T (eq 4) is found to be constant, while with eq 2 the corrected diffusivity is found to become concentration dependent following the relation

$$D_0(\theta) = D_T(1-\theta) = \frac{l^2}{2\tau}(1-\theta) = D_0(\theta=0)(1-\theta) \qquad (6)$$

i.e., to decrease progressively with increasing loading. Equation 6 also stands for the mean-field approach of the self- or tracer diffusivity D, which may be introduced by the relation[1,12,14,21,22]

$$D = \langle y^2(t)\rangle/(2t) \qquad (7)$$

with $\langle y^2(t)\rangle$ denoting the one-dimensional particle mean square displacement during t. The coincidence of the corrected and the self-diffusivity is an immediate consequence of the fact that molecular interaction is only taken into account by excluding multiple site occupancy.[26,27]

Experimental Section

The application of interference microscopy to diffusion studies in nanoporous crystals is based on the fact that the optical density of these crystals is a function of the amount of guest molecules. As a consequence, any change in the local concentration of the crystal under study affects the interference pattern of two light beams, when only one of them passes the crystal and when, subsequently, they are superimposed upon each other (Figure 1d). Thus, changes in the concentration (or, more precisely, in the concentration integral $\int c(x, y, z)\,dz = \langle c(x, y)\rangle_z$ over the concentration in the direction of observation, i.e., in the z-direction; see Figure 1d) appear as a change in the interference pattern.

We have applied a Carl−Zeiss JENAPOL interference microscope with an interferometer of Mach−Zender type. The lateral resolution (in the x- and y-direction), attainable by the device, is on the order of 0.5 μm. The minimum temporal separation between two subsequent concentration profiles is 10 s.

Microporous ($Mn(HCO_2)_2$) crystals, with edge lengths of some tens of microns, have been synthesized following Dybtsev et al. in a steel autoclave with a Teflon-lined insert.[28,29] The crystals contain a one-dimensional channel network which is based upon internal cages with a diameter of 0.55 nm being connected by windows of 0.45 nm (Figure 1b).[29] Figure 1a shows the SEM image of a typical crystal resulting from this synthesis. Figure 1c provides the image of the crystal under study, including its spatial extension and the range (white dots at $x = 41$ μm) of perfect crystallinity considered in this study.

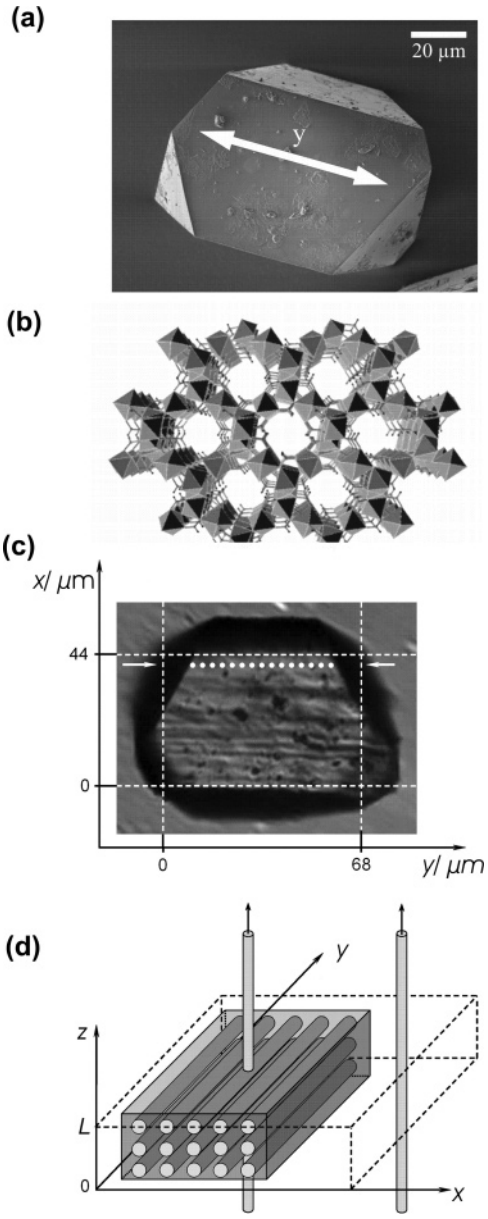

Figure 1. SEM image of a typical ($Mn(HCO_2)_2$) crystal with indicated y-axis (a), scheme of the one-dimensional channel structure of ($Mn(HCO_2)_2$) along y-axis (b),[28] crystal part (white dots at $x = 41$ μm) in which the profiles shown in Figure 3b have been measured (c), and simplified one-dimensional pore structure of ($Mn(HCO_2)_2$) and the measuring principle based on the observation of the interference pattern between the light beams passing the crystal and the surrounding atmosphere (d).

Figure 2 displays the adsorption isotherm, which has been determined for our probe molecule methanol at the temperature of our uptake experiment, 25 °C, by a standard gravimetric device. Included as well into this figure are the best fit of a Langmuir-type isotherm to the experimental data points and the ranges of pressure ($0 < p \le 0.08\ p_0$, with a saturation vapor pressure of $p_0 = 130$ mbar) and loading ($0 < c \le 77$ $mg^{methanol}/g^{MOF}$, corresponding to $0 < \theta \le 0.57$) covered in our uptake experiment under observation by interference microscopy.

Sample preparation before onset of molecular uptake was cared for by activating the crystal at vacuum at 150 °C for 24 h.

(23) Doetsch, I. H.; Ruthven, D.; Loughlin, K. F. *Can. J. Chem.* **1974**, *52*, 2717.
(24) Vavlitis, A. P.; Ruthven, D. M.; Loughlin, K. F. *J. Colloid Interface Sci.* **1981**, *84*, 526.
(25) Garg, D. R.; Ruthven, D. M. *Chem. Eng. Sci.* **1972**, *27*, 417.
(26) Krishna, R.; Paschek, D.; Baur, R. *Microporous Mesoporous Mater.* **2004**, *76*, 233−246.
(27) Krishna, R.; van Baten, J. M. *J. Phys. Chem. B* **2005**, *109*, 6386−6396.
(28) Dybtsev, D. N.; Chun, H.; Yoon, S. H.; Kim, D.; Kim, K. *J. Am. Chem. Soc.* **2004**, *126*, 32−33.
(29) Arnold, M.; Kortunov, P.; Jones, D. J.; Nedellec, Y.; Kärger, J.; Caro, J. *Eur. J. Inorg. Chem.* **2007**, 60−64.

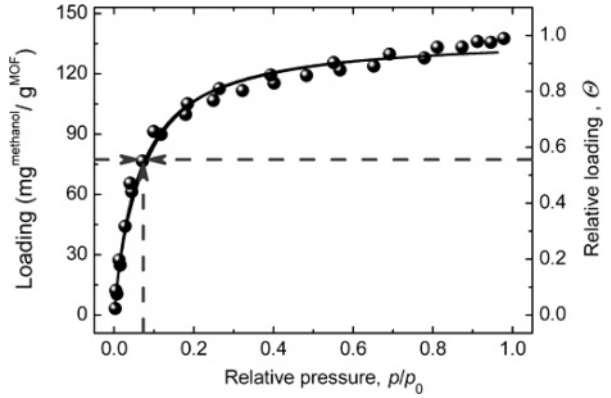

Figure 2. Adsorption isotherms of methanol in $Mn(HCO_2)_2$ at 25 °C. The full line represents the best fit of the isotherm to a Langmuir-type isotherm $c = a\kappa p/p_0/(1 + \kappa p/p_0)$ with $a = 138.57 \pm 1.59$ mg/g and $\kappa = 17.16 \pm 1.01$. Arrows indicate the range of the uptake experiment (pressure step from 0 to 10 mbar).

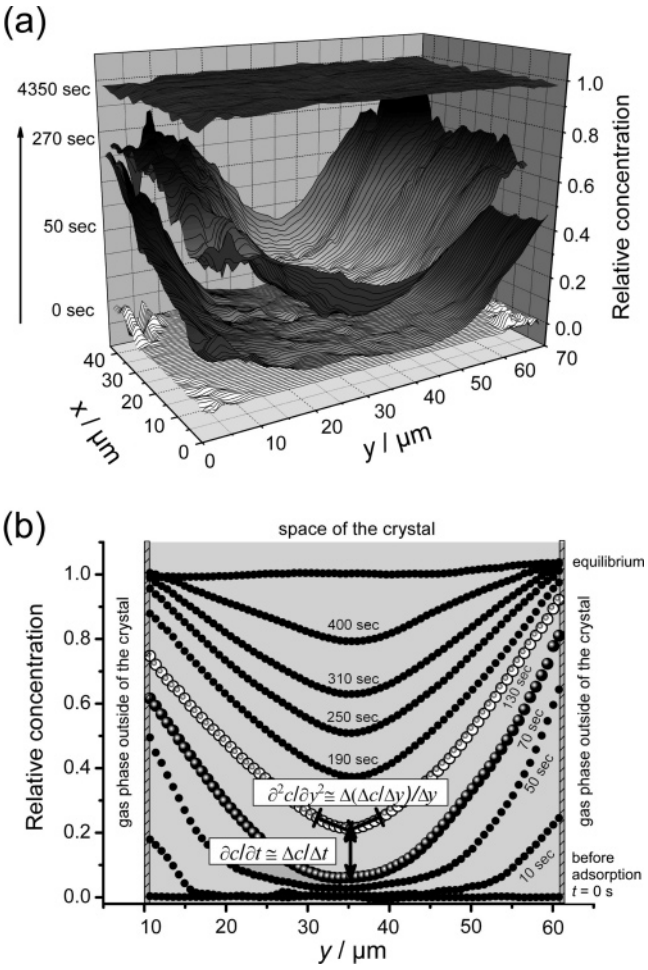

Figure 3. Evolution of the two-dimensional concentration profiles (a) and of the one-dimensional concentration profiles in the y-direction ($x = 41$ μm) (b) of methanol in the MOF crystal for a pressure step from 0 to 10 mbar. The method of evaluating the terms $\partial^2 c/\partial y^2$ and $\partial c/\partial t$ is also indicated.

Results and Discussions

As an example, Figure 3a represents the distribution of methanol within a single crystal of MOF manganese formate, 50 and 270 s after the onset of uptake by enhancing the external methanol pressure from 0 to 10 mbar.

Obviously, considering the total of the crystal, the transient concentration profiles $\langle c(x, y)\rangle_z$ do not reveal the features to be expected for molecular uptake by a perfect, homogeneous crystal. In this case, in view of the one-dimensional channel structure (Figure 1b) one should rather have expected an ideal constancy of concentration in the x-direction, i.e., perpendicular to the channels. The observed deviations, however, are not unusual. In fact, previous application of interference microscopy to a number of host systems, including FER-,[30] MFI-,[31] and AFI-[32] type zeolite crystallites, revealed similar nonideal patterns. They had to be attributed to structural defects. Thus, the host architecture as revealed by transport measurements appeared to be notably different from the ideal text book structure. In one-dimensional channel systems such deviations are particularly likely, since a single obstruction is sufficient to block the whole channel. Therefore, in the given case, it is more remarkable that over an extended range (dotted line in Figure 1c, representing a volume of about $2 \times 50 \times 30$ μm^3 or 10^{12} unit cells)[33] the crystal under study reveals completely regular concentration patterns (symmetric in y-, no variation in x-direction) which can be shown to strictly comply with the behavior expected for one-dimensional lattice gas diffusion. Correspondingly we may imply that within this part of the crystal the concentration $\langle c(x, y)\rangle_z$ resulting from interference microscopy varies neither with z nor with x. Hence, we have direct access to the local concentration $c(y)$.

The corresponding profiles are displayed in Figure 3b. The by far dominating mechanism leading to the temporal change $\partial c/\partial t$ in concentration is brought about by diffusion in the channel direction (i.e., in the y-direction). Therefore, data analysis may be based on the solution of Fick's second law[1,12,14,21,22]

$$\frac{\partial c}{\partial t} = \frac{\partial}{\partial y} D_T \frac{\partial c}{\partial y} = D_T \frac{\partial^2 c}{\partial y^2} + \frac{\partial D_T}{\partial c}\left(\frac{\partial c}{\partial y}\right)^2 \qquad (8)$$

For an ideal, homogeneous system, Fick's second law is expected to describe the evolution of the concentration profiles as shown in Figure 3a with the transport diffusivity $D_T(c)$ as an in general unknown, concentration-dependent coefficient. Hence, $D_T(c)$ may in turn be determined from the microscopic application of eq 8 to the measured spatial-temporal concentration dependence. This procedure is particularly effective in the very center of the profiles (i.e., for $y = 25$ μm), where $\partial c/\partial y = 0$ and the transport diffusivity immediately follows as

$$D_T = \frac{\partial c/\partial t}{\partial^2 c/\partial y^2} \qquad (9)$$

As schematically indicated in Figure 3b, the partial derivatives may be easily deduced from the differences in concentration at subsequent instants of time and from the curvature of the profiles, respectively.

(30) Kärger, J.; Kortunov, P.; Vasenkov, S.; Heinke, L.; Shah, D. B.; Rakoczy, R. A.; Traa, Y.; Weitkamp, J. *Angew. Chem., Int. Ed.* **2006**, *45*, 7846−7849.
(31) Kortunov, P.; Vasenkov, S.; Chmelik, C.; Kärger, J.; Ruthven, D. M.; Wloch, J. *Chem. Mater.* **2004**, *16*, 3552−3558.
(32) Lehmann, E.; Chmelik, C.; Scheidt, H.; Vasenkov, S.; Staudte, B.; Kärger, J.; Kremer, F.; Zadrozna, G.; Kornatowski, J. *J. Am. Chem. Soc.* **2002**, *124*, 8690−8692.
(33) Garberoglio, G.; Skoulidas, A.; Johnson, J. K. *J. Phys. Chem. B* **2005**, *109*, 13094−13103.

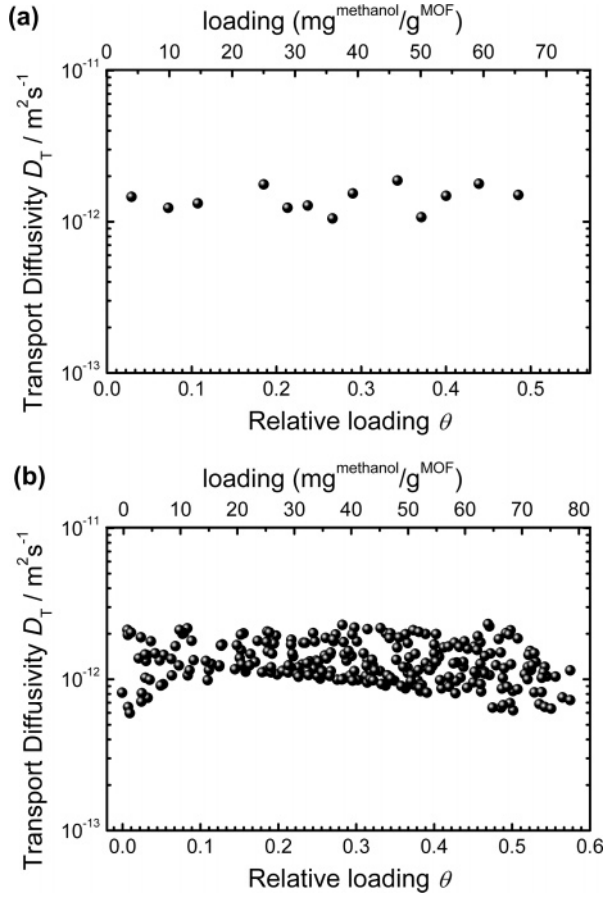

Figure 4. Concentration dependence of the transport diffusivity as determined from the center (a) and from the entire profile (b).

Figure 4a displays the concentration dependence of the diffusivities determined via eq 9 in the center of the profiles. The fact that the obtained diffusivities are essentially constant over the whole concentration range notably facilitates exploiting the total information contained in the concentration profiles for exploring intracrystalline transport diffusion. As a consequence of this constancy, the magnitude of $\partial D_T/\partial c$ can only attain very small values. Therefore, the second summand on the right-hand of eq 8 can also be omitted outside of the crystal center, i.e., for nonvanishing values $\partial c/\partial y$. Consequently, eq 9 turns out to be applicable for the total profiles! Figure 4b shows the entity of the thus determined diffusivities. Within the relatively broad range of scattering which is inherent to this type of microscopic data analysis, there is no indication of a deviation of the diffusivities from their mean value of $D_T = (1.5 \pm 0.4)\ 10^{-12}$ m^2 s^{-1} over the whole concentration range.

The evidence of our results would be additionally confirmed by comparing the experimentally observed evolution of the concentration profiles with the corresponding solution of Fick's second law, based on the microscopically determined diffusivities. In view of the constancy of this diffusivity, such a comparison might be expected to be easily performed by means of standard analytical solutions of molecular uptake and release, as compiled, e.g., in ref 34. However, in addition to the relevant diffusivities, the shape of the concentration profiles may as well be determined by the permeability through the crystal surface. Inspection of the concentration profiles provided by Figure 3 reveals a substantial divergence between boundary concentrations on either side of the crystal and the equilibrium concentrations. Only 310 s after the onset of adsorption, the boundary concentration is found to coincide with the equilibrium value. This is an unequivocal indication of the existence of surface barriers, i.e., of finite surface permeabilities, since heat effects may be shown to be ruled out.[35] It is true that ref 34 also contains analytical solutions for the combined influence of intracrystalline diffusion and surface resistances. However, they imply that, besides the intracrystalline diffusivity, also the surface permeability has to be constant.

Besides microscopically exploring intracrystalline diffusivities, interference microscopy as well proves to be the first technique to provide detailed, microscopic information about the magnitude of the surface permeabilities. Following,[34] the surface permeability α is defined by the equation

$$j = \alpha(c_{eq} - c_{surf}(t)) \tag{10}$$

where c_{eq} is the equilibrium concentration and $c_{surf}(t)$ denotes the concentration close to the crystal surface (i.e., the boundary concentration) at time t. The flux density j results from the uptake per time following the relation

$$j = \frac{1}{2A}\frac{dm}{dt} = \frac{1}{2A}\frac{d(\int_A \int_{-l}^{l} c(y)\, dy)}{dt} \tag{11}$$

where $m(t)$ denotes the total uptake at time t by the entire crystal, l is the half length of the crystal extension in the channel direction, and A stands for the area of the crystal phase perpendicular to the channels. Combining these two equations yields

$$\alpha = \frac{dm/dt}{c_{eq} - c_{surf}(t)} \tag{12}$$

and hence the option to determine the surface permeabilities from data accessible, in principle, by interference microscopy. One has to have in mind, however, that, due to the generally inevitable structural imperfections close to the crystal boundaries, concentrations accessible by interference microscopy toward the crystal margins do not coincide with the actual values of $c_{surf}(t)$ as appearing in eq 12. Thus, in the present case of molecular uptake, the concentrations measured at the crystal margins will be below the correct value of $c_{surf}(t)$, so that the real permeabilities have to be expected to be systematically larger than the permeabilities following form eq 12. Figure 5 displays these data. Most remarkably, in contrast to the intracrystalline diffusivity which remains constant over the total range of concentration, the surface permeability is found to significantly increase with increasing concentration. Only by means of interference microscopy this type of information has become experimentally accessible. There is clearly no reason to assume that surface permeabilities should not deviate from diffusivities based on the quite general feature that they may depend on concentration. Since they are brought about by different mechanisms one may also accept that, as in the given case, one of these quantities (here the permeability) varies with varying concentration while the other (the transport diffusivity)

(34) Crank, J. *The Mathematics of Diffusion*; Clarendon Press: Oxford, 1975.

(35) Heinke, L.; Chmelik, C.; Kortunov, P.; Shah, D. B.; Brandani, S.; Ruthven, D. M.; Kärger, J. *Microporous Mesoporous Mater.*, in press.

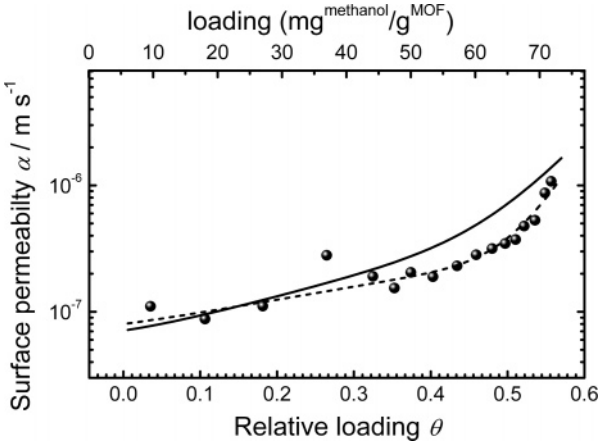

Figure 5. Surface permeability of the MOF-type crystal under study during methanol uptake as a function of the boundary concentration (mean value during the considered time step), following from the application of eq 12 with the boundary concentration $c_{surf}(t)$ taken from the margins of the measured concentrations. The polynomial fit to these data is given by the broken line. The full line shows that dependence of the permeability on concentration which leads to the best fit of the recalculated concentration profiles to the experimental ones (Figure 6).

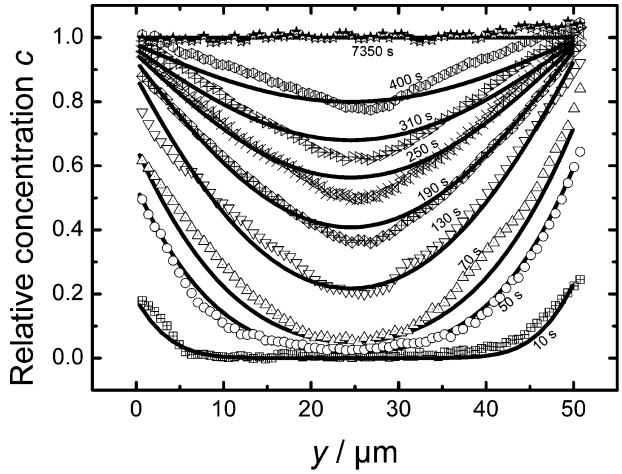

Figure 6. Comparison of the transient concentration profiles during methanol uptake by the MOF-type crystal as recorded by interference microscopy (symbols) with the corresponding profiles recalculated from the measured diffusivities with surface permeabilities (full line in Figure 5) which lead to the best fit to the experimental points.

remains constant. After these very first steps in exploiting interference microscopy to determine a so far inaccessible quantity, we would like to abstain from premature speculations on possible mechanisms behind this dependency. There is no doubt, however, that their exploration is an attractive task for further studies, with respect to both their practical consequences and a better understanding of the fundamentals of mass transfer at the interface between the sorbed and gaseous phases.

As the main message of these measurements, relevant in the present contents, we have to note that the surface permeability notably varies during the uptake process. This excludes the option to predict the evolution of the concentration profiles by analytical expressions. Instead, we have used a finite difference solution algorithm.[34,36] This allows a straightforward numerical calculation of the evolution of the intracrystalline concentration profiles on the basis of the (microscopically determined) experimental data for the transport diffusivity ($D_\Gamma = 1.5 \times 10^{-12}$ $m^2\ s^{-1}$) and the surface permeability. As an analytical expression leading to the best polynomial fit of the measured concentration profiles, we have used the relation $\alpha = (7.1 + 8.5\ c + 24.5\ c^2 + 9.7\ c^4 + 61.1\ c^8 + 53.5\ c^{12}) \times 10^{-8}$ m s^{-1} (full line in Figure 5). In agreement with our considerations following eq 12, these permeability data are slightly above those determined via eq 12 with the boundary concentrations attainable by interference microscopy. Simultaneously, they characterize the range of uncertainty in which the actual surface permeabilities are to be expected. Figure 6 displays the thus obtained concentration profiles in comparison with the experimental data resulting from an analysis of the interference patterns. Though there is no ideal agreement, the calculated concentration profiles are found to follow the experimental data over the whole uptake process with deviations typically below a value of 20%. Never before has such a comparison been possible. Different factors might have given rise to the appearing differences, including the uncertainty in the measured concentrations (±2% of final concentration), residual lattice imperfection, and deviations from the uniformity in the surface permeability which is implied by the use of the boundary condition on the basis of the (macroscopic) eq 10.

Conclusion

Over decades, researchers have been concerned by the fact that the transport diffusivities resulting from macroscopic uptake and release experiments significantly vary with concentration.[21,22] In processes covering large concentration ranges such a behavior clearly notably impedes the option of their analytical treatment. Though there were some particular exceptions where, e.g., the transport diffusivities remained constant,[37] in numerous cases the concentration dependence of the transport diffusivity was found to be that of the so-called thermodynamic factor $\partial \ln p/\partial \ln \theta$, i.e., of the logarithmic derivative of the adsorption isotherm $\theta(p)$. In this way, by representing the transport diffusivity as the product of this derivative and a so-called corrected diffusivity D_0 (see eq 5), a novel transport parameter has been defined, which was assumed to much better comply with the requirement of constancy. Recently, coherent QENS[9] opened up a novel route to a direct measurement of transport diffusivities. It is based on the observation of the local fluctuations of the sorbate density. Besides some cases revealing satisfactory agreement with the supposition of the constant corrected diffusivity (as for N_2 and CO_2 in silicalite-1[38]), these measurements also indicate notable deviations from this rule. For ethane[39] and CF_4[8] in silicalite-1, the transport diffusivity increases by roughly the same factor with increasing loading as the corrected diffusivity decreases. For *n*-hexane in silicalite-1[40] the transport diffusivity is even closer to constancy than the corrected diffusivity.

After reporting transport diffusivities which increase over close to 2 orders of magnitude with increasing concentration,[30,31] the present application of interference microscopy to methanol in MOF manganese formate reveals a constant value of (1.5 ±

(36) Heinke, L. Diploma thesis, 2006.

(37) Qureshi, W. R.; Wei, J. *J. Catal.* **1990**, *126*, 147−172.
(38) Papadopoulos, G. K.; Jobic, H.; Theodorou, D. N. *J. Phys. Chem. B* **2004**, *108*, 12748−12756.
(39) Chong, S. S.; Jobic, H.; Plazanet, M.; Sholl, D. S. *Chem. Phys. Lett.* **2005**, *408*, 157−161.
(40) Jobic, H.; Laloue, N.; Laroche, C.; van Baten, J. M.; Krishna, R. *J. Phys. Chem. B* **2006**, *110*, 2195−2201.

$0.4) \times 10^{-12}$ m^2 s^{-1} from zero loading up to a pore filling factor of over 0.5. Never before could such constancy be detected by the direct measurement of transport diffusion over such an extended range of concentrations. In addition, as illustrated by Figure 2, the equilibrium sorption data are nicely reflected by the Langmuir isotherm. Thus, methanol in MOF manganese formate is found to follow in two features the behavior expected for a one-dimensional lattice gas.

Being able to monitor the evolution of the total concentration profiles, interference microscopy is also able to directly determine the permeability of the crystal surface. It turns out that this permeability is by far not enough to allow immediate equilibrium between the actual boundary concentration and the equilibrium value corresponding to the pressure in the external gas phase. Most interestingly, though intracrystalline transport diffusion is found to be constant over the whole range of concentrations covered in the experiment, over the same range of concentrations the surface permeability increases by an order of magnitude. The deeper exploration of the nature of the surface barrier as revealed by such permeability studies is doubtlessly among the most fascinating tasks of further research by interference microscopy.

Acknowledgment. Financial support by the German Science Foundation, by the European Commission (INSIDE-POReS), and by Fonds der Chemischen Industrie is gratefully acknowledged. We are particularly obliged to two referees for helpful criticism and stimulating suggestions.

JA071265H